






Vegetation resilience does not increase consistently with greening in China's Loess Plateau

Zhuangzhuang Wang ^{1,2}, Bojie Fu ^{1,2}✉, Xutong Wu³, Yingjie Li ⁴, Yuhao Feng ⁵, Shuai Wang ³, Fangli Wei^{1,2} & Liwei Zhang⁶

Recent concurrent processes of vegetation greening and reduced resilience (the capacity to recover from disturbances) worldwide have brought many uncertainties into sustainable ecosystems in the future. However, little is known about the conditions and extent to which greening affects resilience changes. Here we assess both vegetation dynamics and resilience in China's Loess Plateau from 2000 to 2020 using satellite-based vegetation data and an early warning indicator. Our results reveal an overall greening trend in vegetated areas, while resilience shifted from gains to losses at a breakpoint in 2010. Vegetation greening generally contributed to resilience gains, whereas increased temperature and precipitation variability contributed to the resilience loss observed in 2011–2020. These findings provide empirical evidence that vegetation greening does not necessarily correspond to an increase in resilience. We therefore recommend integrating resilience indicators into ecological restoration and conservation efforts to gain a more comprehensive understanding of vegetation states and support effective ecosystem stewardship.

¹State Key Laboratory of Urban and Regional Ecology, Research Center for Eco-Environmental Sciences, Chinese Academy of Sciences, 100085 Beijing, China. ²University of Chinese Academy of Sciences, 100049 Beijing, China. ³State Key Laboratory of Earth Surface Processes and Resource Ecology, Faculty of Geographical Science, Beijing Normal University, 100875 Beijing, China. ⁴Natural Capital Project, Stanford University, Stanford, CA 94305, USA. ⁵Institute of Ecology, College of Urban and Environmental Sciences, Peking University, 100871 Beijing, China. ⁶School of Geography and Tourism of Shaanxi Normal University, 710119 Xi'an, China. ✉email: bfu@rcees.ac.cn

Terrestrial vegetation plays a crucial role in regulating the exchange of carbon, water, and energy between the land and the atmosphere^{1,2}. It provides valuable ecosystem services such as carbon storage and soil conservation that support human well-being³. Long-term satellite data have revealed a significant global greening trend in vegetated areas since the 1980s, driven primarily by human land-use management (e.g., revegetation in China), climate change and CO₂ fertilization^{2,4}. The persistence and functionality of vegetation ecosystems are highly tied to their capacity to withstand and recover from natural and human-induced perturbations (i.e., their resilience)⁵. However, recent studies suggest that the changing climate has reduced vegetation resilience worldwide^{5–8}, particularly in critically valuable tropical forests^{9–11}. Concurrent processes of vegetation greening and resilience loss raise uncertainties regarding the future of vegetation ecosystems¹². Yet, empirical relationships between vegetation dynamics and changes in resilience have not been well investigated. Key questions remain regarding the specific conditions and extent to which vegetation greening may contribute to resilience changes¹³. Addressing these knowledge gaps is vital for gaining a comprehensive understanding of the dynamics that shape terrestrial plant ecosystems and for formulating effective management strategies^{6,12}.

Vegetation greening (or browning) at a location refers to statistically significant increases (or decreases) in average leaf size, plant density, or changes in species composition². Traditional studies on vegetation dynamics primarily focus on smooth and monotonic changes in vegetated ecosystems¹⁴. However, these methods solely represent the mean state of a system and may not reflect the non-linear dynamics underpinning resilience¹¹. Higher-order statistical characteristics that respond more sensitively to destabilization than the mean are urgently needed to quantify resilience^{11,15}. A promising approach to address this challenge is the use of early warning indicators (EWIs) to detect critical transitions^{16,17}. Theoretical and empirical studies have shown that a loss of resilience can be identified through increased temporal autocorrelation and variance in the state of a system^{7,18,19}. These indicators reflect a decline in recovery rates due to the critical slowing down of system processes that occur at thresholds^{18–20}. By applying the EWIs with satellite-based vegetation indices, recent studies have reported the emerging signals of reduced resilience in vegetated areas globally, indicating a high risk of abrupt transition when facing external disturbances^{5–7,11}.

Intuitively, vegetation greening, such as increased vegetation productivity and density, is often associated with improved physiological functions that can enhance vegetation's capacity to withstand and recover from disturbances⁵. However, concurrent observations of global vegetation greening^{2,4} and signals of declined vegetation resilience worldwide^{5–7,9,11} suggest that vegetation greening does not necessarily correspond to an increase in resilience. Opposite changes between vegetation dynamics and resilience can arise from various factors. First, when greening is dominated by a single plant species and/or exotic species, vegetated ecosystems may experience declined resilience due to reduced functional and response diversity and maladaptation of exotic species to local conditions^{21–25}. Second, the presence of greener vegetation does not necessarily indicate the overall health of an ecosystem, as it is constrained by the carrying capacity of the system itself^{26–28}. The biogeophysical effects of greening can negatively impact vegetation growth conditions^{2,29}. For instance, in drylands with limited water availability, dense vegetation and greening can deplete large amounts of soil moisture and thus alter surface-water availability^{26,29–31}. This can potentially increase drought occurrence and create a positive feedback loop between drying and vegetation degradation³². Third, the positive effects of greening

on resilience can be offset by climate change-induced alterations in background climate and increased climate variability^{5,6}. These factors highlight the complex and context-dependent relationships between vegetation dynamics and resilience changes in a changing world.

Resilience assessments can complement traditional studies on vegetation dynamics, particularly when conducting ecological restoration work³³. While scientists and policymakers often focus on the greening levels of vegetation ecosystems, their resilience has been largely neglected^{33,34}. Neglecting resilience can lead to unexpected consequences. For instance, despite short-term increases in vegetation cover and greenness, resilience loss can result in forest dieback and sudden increases in tree mortality when even a small disturbance is encountered^{12,35}. Understanding and identifying the controlling factors of vegetation resilience is important for implementing targeted protection and management policies for vegetated ecosystems^{6,36}. Recent studies have shown that vegetation resilience tends to be greater in regions with higher water availability and is lower in regions with more pronounced inter-annual precipitation variability^{5,10,36}. However, previous studies primarily used the space-for-time method to analyze the controlling factors of vegetation resilience, and few factors were considered in the analyses^{10,36}. The temporal correlations of resilience with multifaceted climatic factors and their relative importance have received less attention.

The Loess Plateau in China is an ecologically vulnerable area that has experienced severe vegetation loss, soil erosion, and land degradation³⁷. Efforts to restore the degraded ecosystems have been undertaken by the Chinese government since the 1970s, with the implementation of various landscape engineering and ecological restoration measures³⁸. Among these measures, the Grain for Green project, initiated in 1999, has proven particularly successful³⁹. This project aims to prevent soil erosion, alleviate flooding, and store carbon by increasing forest and grassland cover on previously cropped hillslopes, as well as converting cropland, barren hills, and wasteland into forested areas⁴⁰. Over the past two decades, ecological restoration efforts have resulted in a visible “greening” trend across the Loess Plateau^{41–43}, with the vegetation cover increasing from 32% in 1999 to 64% in 2019⁴⁴. However, to our knowledge, studies on vegetation resilience have not been conducted, limiting the comprehensive understanding of changes in the vegetation states.

In this study, we aim to assess both vegetation dynamics and resilience change in China's Loess Plateau to determine if greening is accompanied by an increase in resilience. To measure vegetation resilience, we used the temporal changes of the lag-1 autocorrelation (AR(1))¹⁹. This metric was calculated in sliding windows from the detrended and deseasonalized monthly kNDVI (kernel Normalized Difference Vegetation Index; a recently improved vegetation index) data from February 2000 to December 2020^{11,36,45} (Methods). We then analyzed the spatial correspondence of the tendency of vegetation dynamics and resilience metric AR(1), as well as their temporal correlations. In addition, we conducted an attribution analysis to investigate the effects of environmental factors on resilience changes and their relative importance.

Results

Inconsistency of vegetation dynamics and resilience change.

Averaged across the Loess Plateau, we observed an increasing trend in mean kNDVI values ($\tau = 0.991$, $P < 0.001$) (Fig. 1a), indicating an overall greening of vegetation. The spatial distribution of the kNDVI tendency showed that more than 80% of vegetated grids had experienced greening over two decades (Figs. 1b, 2b, c). However, it is important to note that vegetation

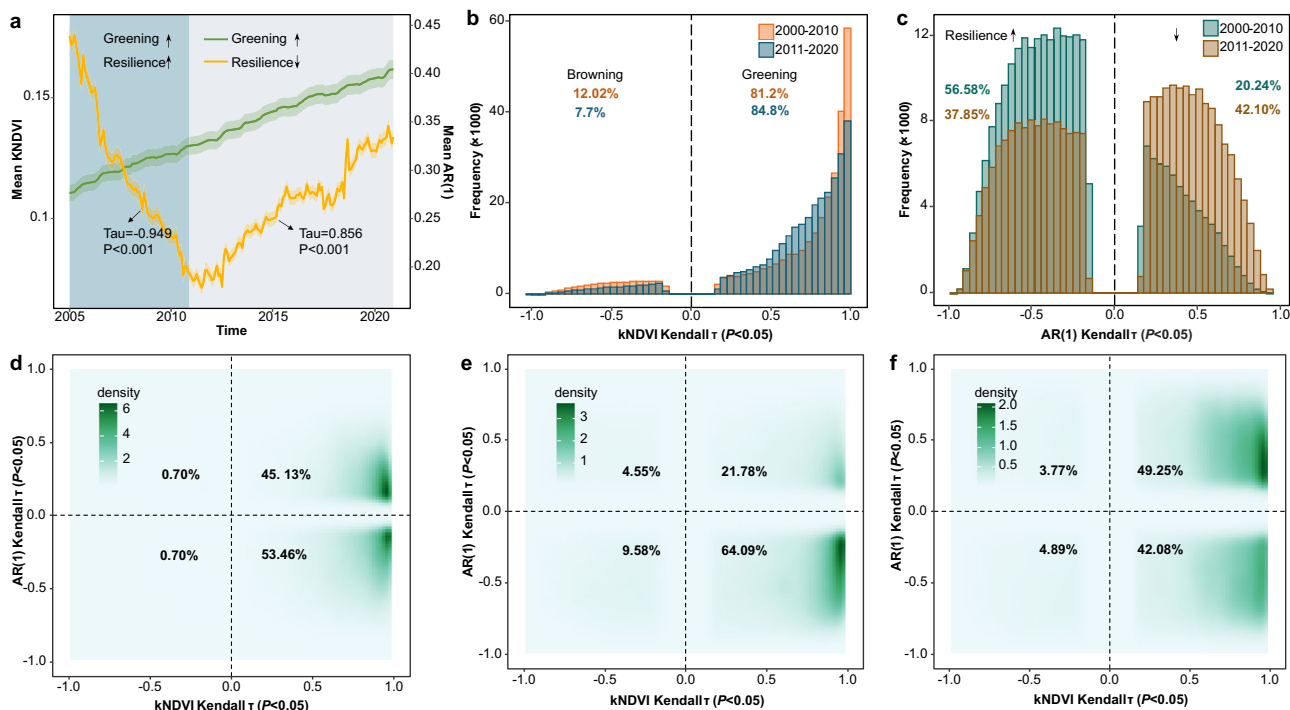


Fig. 1 Temporal patterns of vegetation dynamics and resilience across 2000–2020 and between decade 2000–2010 and 2011–2020. **a** Temporal trajectories of vegetation dynamics and resilience. Continuous lines refer to the regional mean kNDVI (green) and AR(1) (orange), and shaded areas represent the corresponding 95% confidence interval magnified by a factor of 10 for visual purposes. For comparison, the kNDVI values are calculated as the mean using the same 5-year sliding window as AR(1). Note that the mean kNDVI and AR(1) values are plotted at the end of each sliding window. **b** and **c** Histogram of grid-level Kendall τ values for the kNDVI and AR(1) time series, respectively, comparing data for the first decade (2000–2010) and the second (2011–2020). **d–f** Cumulative density distribution of the relationship between kNDVI Kendall τ and AR(1) Kendall τ at the grid scale from 2000–2020 (**d**), 2000–2010 (**e**), and 2011–2020 (**f**). Number labels in four quadrants represent the percentage of pixels of a certain quadrant. Grid cells with non-significant Kendall τ ($P > 0.05$) were not included in the figures for visual purposes.

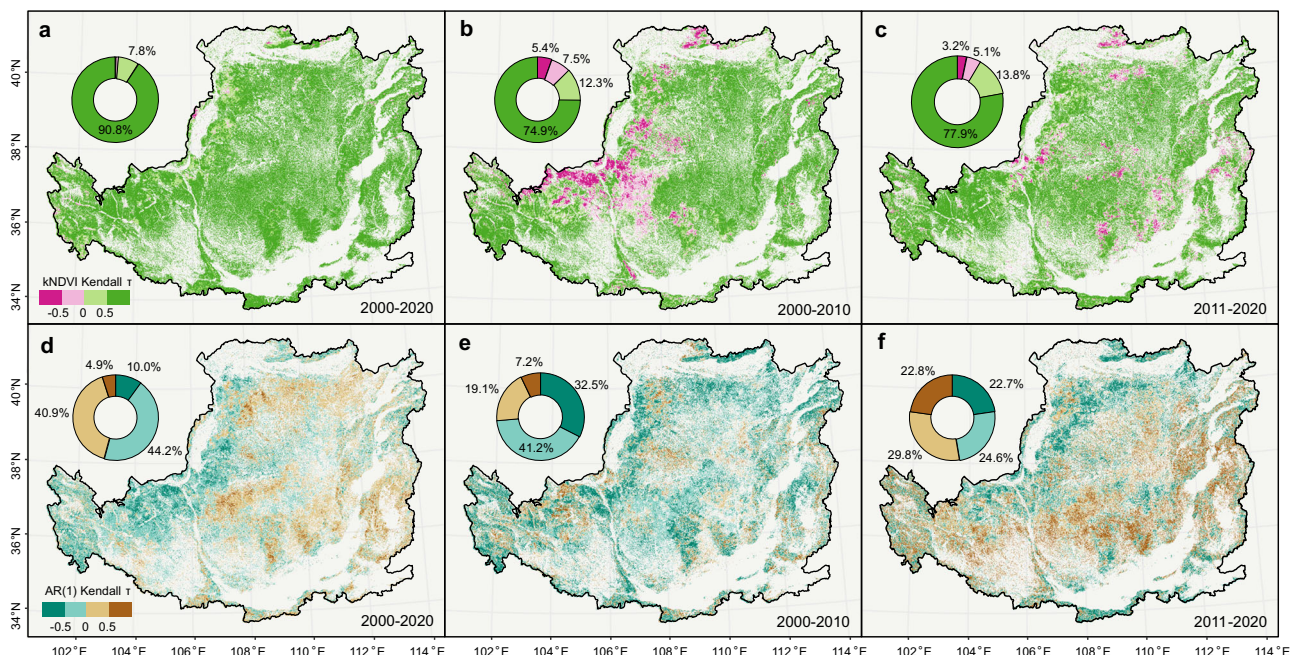


Fig. 2 Spatial patterns of vegetation dynamics and resilience change in 2000–2020, 2000–2010, and 2011–2020. **a–c** Spatial map of the temporal trend in kNDVI values. Positive kNDVI Kendall τ values suggest an increase in kNDVI values and thus greening, and negative kNDVI Kendall τ values suggest browning. **d–f** Spatial map of the temporal trend of AR(1) values. Positive AR(1) Kendall τ values suggest a decline in resilience, and negative AR(1) Kendall τ values suggest an increase in resilience. Grid cells with non-significant Kendall τ ($P > 0.05$) were not included in the figures for visual purposes.

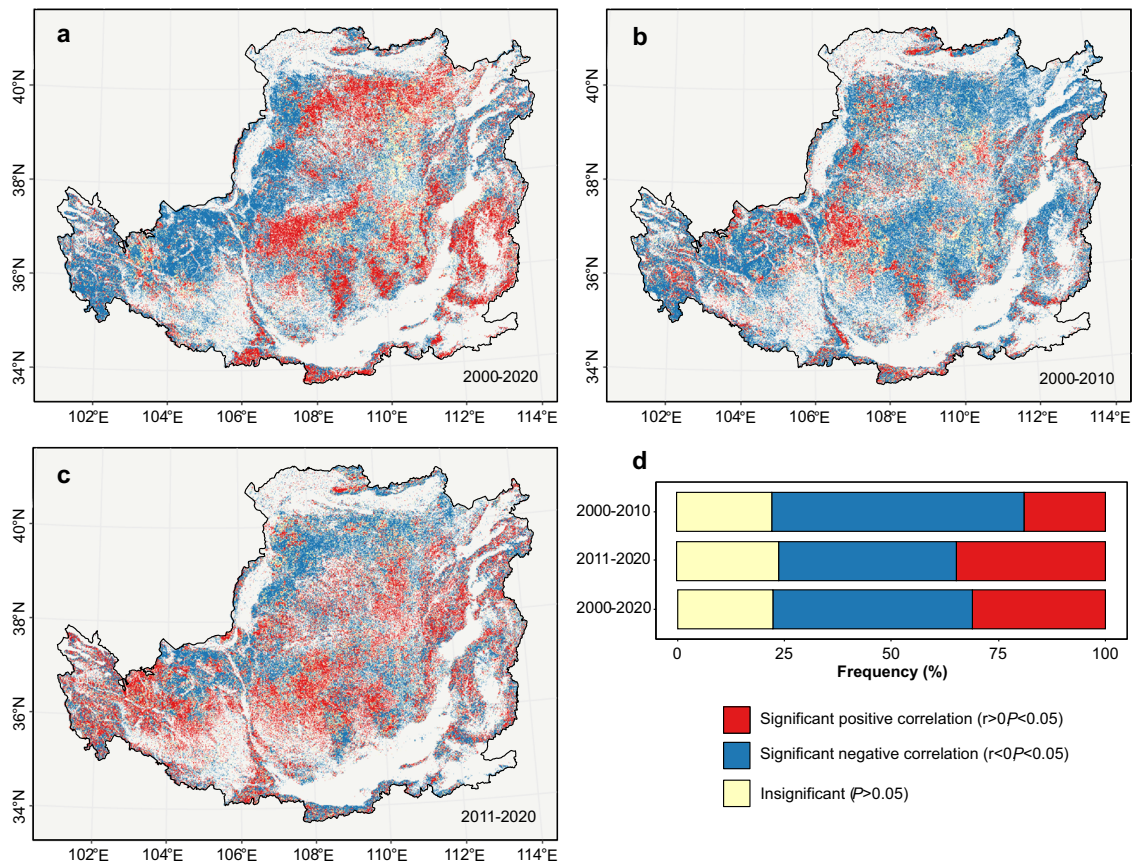


Fig. 3 Correlations between vegetation dynamics (kNDVI time series) and resilience (AR(1) time series). **a–c** Spatial maps of correlation over 2000–2020, 2000–2010, and 2011–2020, respectively. **d** The cover fractions of each correlation type.

resilience did not increase consistently in parallel with greening. The mean AR(1) time series showed a transition from a negative trend ($\tau = -0.949$, $P < 0.001$) to a positive trend ($\tau = 0.856$, $P < 0.001$) at the breakpoint in December 2010, representing a shift from resilience gains to resilience losses (Fig. 1a). Notably, a higher proportion (42.1%) of vegetated grids experienced resilience loss in the second decade (2011–2020) compared to the first decade (20.24%, 2000–2010) (Figs. 1c, 2e, f).

These findings on resilience signals are robust as they are based on data from a single sensor (the Moderate Resolution Imaging Spectroradiometer—MODIS) and a recently improved vegetation index (kNDVI)^{5,45}. We validated the reliability of these resilience signals by employing alternative methods for detrending the kNDVI time series and varying the window length for calculating the AR(1) (Supplementary Figs. 3–5). Remarkably, when using variance as the resilience metric instead of AR(1), similar transitions from widespread resilience gains to resilience losses were observed (Supplementary Figs. 6, 7). These consistent signals provide substantial evidence for notable trajectories in vegetation resilience, which are intimately linked to the stability and sustainability of vegetation ecosystems.

Examination of the spatial correspondence between vegetation dynamics (greening and browning) and resilience change revealed that in the first decade, 64.09% of vegetated grids exhibited a positive kNDVI trend coupled with a negative AR(1) trend (Fig. 1e). This indicates that a considerable portion of vegetated areas experienced both greening and an increasing in resilience. However, in the second decade, this proportion decreased to 42.08%, which was less than the proportion of vegetated grids (49.25%) that exhibited both greening and resilience loss (Fig. 1f). The temporal correlations between the

kNDVI and AR(1) time series mirrored the spatial correspondence of their trend (Fig. 3), validating the finding that the relationship between vegetation dynamics and resilience has changed over the study period. The proportion of vegetated grids with a significant negative correlation ($P < 0.05$) between kNDVI and AR(1), indicating concurrent vegetation growth and increased resilience or vice versa, decreased from 59.1% in the first decade to 41.43% in the second decade (Fig. 3d). Overall, our results suggest an inconsistency between vegetation dynamics and resilience change.

Potential climatic drivers of vegetation resilience change. The areas exhibiting declined resilience (i.e., increasing AR(1) tendency) were predominantly found in semi-arid and dry sub-humid regions with an annual precipitation range of 391 mm–620 mm (Fig. 4). To explore the drivers of vegetation resilience, particularly the causes of resilience loss in the second decade (Figs. 1c, 2f), we conducted a multiple linear regression analysis to assess the effects of climatic factors and their relative importance (Fig. 5). Their spatial patterns were shown in Supplementary Figs. 8, 9. Negative regression coefficients indicate inversely proportional relationships between climatic factors and AR(1) values, that is, scenarios where an increase in a climate variable had a commensurate decrease in AR(1), meaning it improved resilience.

Mean precipitation showed an overall positive effect on vegetation resilience across both decades (Fig. 5a), especially in the second decade (75.66% of vegetated grids), implying that areas with higher precipitation tended to become more resilient over time. However, the relative importance of mean

precipitation in explaining resilience change declined in 60.34% of vegetated grids during the second decade (Fig. 5b), suggesting the influence of other climatic factors. On average, the mean temperature had a negative effect on vegetation resilience in a larger number of areas during the second decade, with its relative importance increasing in 53.99% of vegetated grids (Fig. 5). This observation could be attributed to the elevated mean temperature observed during this period (Supplementary Figs. 10, 11).

Overall, precipitation variability and temperature variability had a negative impact on vegetation resilience (Fig. 5a). Interestingly, the relative importance of precipitation variability increased in 57.85% of vegetated grids from the first to the second decade (Fig. 5b). The potential evapotranspiration showed a shift from a negative to a positive effect on vegetation resilience, with its relative importance increasing in 62.18% of vegetated grids. Moreover, the aridity index, commonly used to measure water availability, had an overall negative effect on vegetation resilience, with negative effects observed in 68.08% of vegetated grids in the second decade (Fig. 5a). These findings suggest that more areas with high evapotranspiration and aridity, indicating low water availability, increased in resilience, which aligns with the observed spatial changes in resilience (Fig. 4a, b).

Discussion

The persistence and functionality of vegetation ecosystems are crucial for global and regional development, as they contribute to climate change mitigation and provide essential ecosystem services^{2,5}. Our study reveals an overall greening trend in the vegetated land of the Loess Plateau from 2000 to 2020 (Fig. 1a). However, we observed a shift in resilience from gains to losses at a breakpoint in December 2010 (Fig. 1a). Importantly, in the second decade, a larger proportion of vegetated grids experienced both greening and resilience loss (Figs. 1d–f, 3). This study expands upon previous research that has focused solely on vegetation dynamics or resilience by providing empirical evidence that greening does not necessarily correspond to an increase in resilience^{2,4,7,10,11,36}. Our results highlight the value of resilience indicators in capturing important information about vegetation states that cannot be identified through simpler methods that characterize the mean state of a system. Consequently, we recommend integrating resilience indicators into assessments of ecological restoration effectiveness to achieve more comprehensive ecosystem stewardship.

Low-resilience ecosystems are highly vulnerable to environmental perturbations and tend to have slower recovery rates after

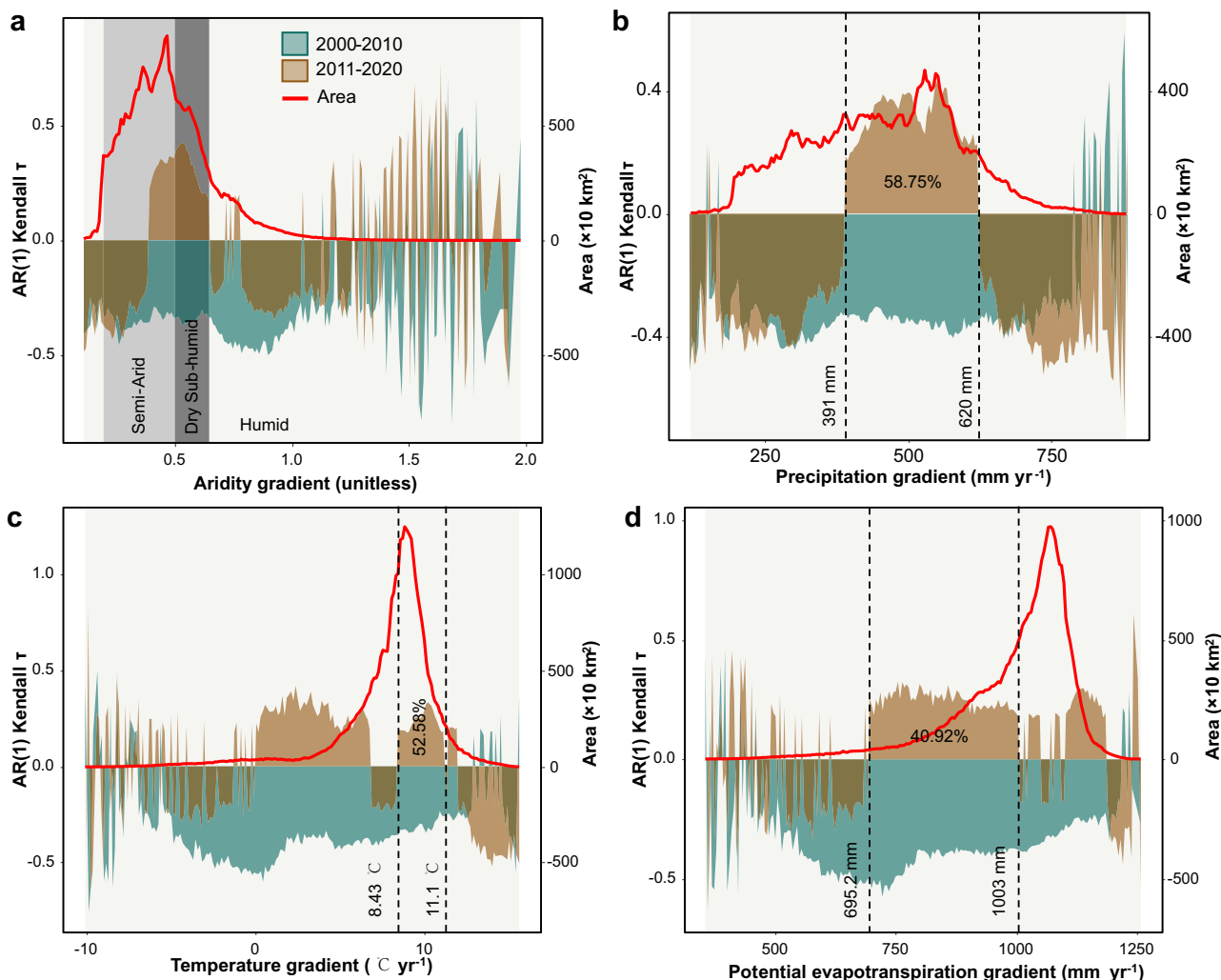


Fig. 4 Changes in vegetation resilience along gradients of climatic factors. Climate factors are the annual mean values from 2000 to 2020 and they were divided into 50 gradients. The y-axis on the left is the median value of AR(1) Kendall τ within each gradient. **a** Aridity gradient. The aridity index was calculated as precipitation divided by potential evapotranspiration. Shaded bars represent several binned groups: Semi-arid (0.2–0.5), Dry sub-humid (0.5–0.65), and Humid (>0.65). **b** Precipitation gradient. **c** Temperature gradient. **d** Potential evapotranspiration gradient. Grid cells with non-significant Kendall τ ($P > 0.05$) were not included in the figures.

disturbances, increasing the risk of a critical transition to an alternative state⁶. Recent studies suggest the temporal loss of resilience can serve as an early warning signal for predicting forest mortality⁴⁶. In our research, we have used high-resolution satellite data to identify several regions where resilience has decreased despite increases in greening, particularly in the last decade (Fig. 2). In light of the extensive greening observed in the Loess Plateau, recent research has emphasized the importance of prioritizing efforts to enhance the stability and sustainability of vegetated ecosystems to preserve the achievements of ecological restoration^{37,39}. Our findings provide supportive evidence for this argument from a resilience perspective, and they also offer valuable insight for informing future ecological restoration policies by identifying regions with resilience loss that require special attention and protection.

It is important to acknowledge the potential and limitations of the resilience indicators used in this study^{6,16,47}. The resilience indicators (AR(1) and variance) build upon the theory of “critical slowing down” and can be used to estimate resilience in situations where controlled experiments are not feasible and external perturbations are infrequent, particularly in the context of large-scale ecosystems^{7,16}. These indicators rely on readily available long-term satellite-based vegetation index datasets⁴⁸. In particular, recent studies have provided evidence supporting the use of AR(1) and variance as metrics for assessing vegetation resilience by comparing them with empirically estimated recovery rates following disturbances^{7,36}. However, it is crucial to recognize that the resilience signals detected by the “critical slowing down” indicators should be viewed as early warning tools rather than precise predictors of critical transitions⁴⁷. The occurrence of resilience loss does not necessarily imply that these regions will undergo immediate critical transitions⁴⁷. To enhance the practical value and policy relevance of resilience indicators, further

research is needed to investigate the predictive relationship between these indicators and specific critical vegetation transitions⁵. This will contribute to a more comprehensive understanding of resilience dynamics and provide valuable insights for future decision-making processes.

Our results demonstrated that greening does not always correspond to an increase in vegetation resilience or both are not simply linearly related. In the first decade, a large portion (64.09%) of the vegetated area experienced both greening and an increase in resilience (Fig. 1e). This result is further supported by temporal correlations between mean kNDVI and AR(1), where negative correlations were observed in 59.1% of the vegetated grids during the first decade (Fig. 3d). The increased vegetation resilience coinciding with greening in the first decade is probably due to enhanced plant productivity, improved habitat conditions given a specific period, and reduced anthropogenic disturbances resulting from ecological protection policies^{5,11}. However, it is important to discuss why there is a shift from widespread resilience gains to losses from the first decade to the second decade along with greening (Figs. 1c, 2f). Considering the influence of climatic factors on resilience and their changing relative importance, our findings indicate that increasing precipitation variability and increasing temperature likely contributed to the resilience loss in the second decade (Fig. 5). A recent study has reported that regions with higher water availability tend to exhibit greater vegetation resilience, whereas areas with pronounced precipitation variability show lower resilience³⁶. Since the Loess Plateau is largely located in semi-arid regions, water availability is the main limiting factor for vegetation health and growth³⁷. The combination of evaporation, transpiration exacerbated by a warming climate, and increasing precipitation variability can intensify water scarcity, thus impairing physiological functions and the ability of vegetation to adapt to disturbances such as droughts^{5,10,36}.

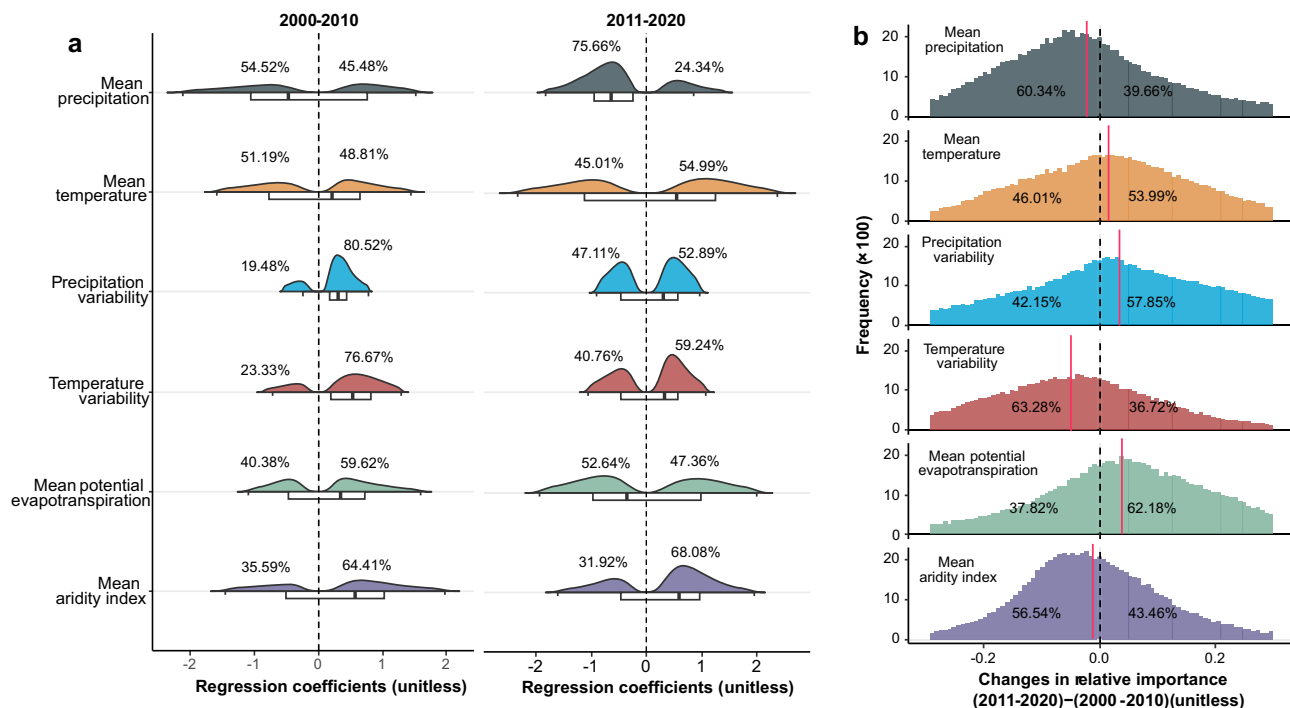


Fig. 5 Relative importance of climatic factors and their effects on vegetation resilience. **a** Frequency distribution of the effects of climatic factors (i.e., regression coefficients) on vegetation resilience (i.e., AR(1) values) over 2000–2010 and 2011–2020. The explanatory variables were scaled using the `scale()` function in R and therefore the regression coefficients are unitless and comparable. **b** Frequency distribution of the differences in the relative importance of climatic factors for two independent decades (2011–2020 minus 2000–2010). The number labels refer to the percentage of the observations that are lower and higher than zero. The red line in **(b)** is the mean value. Grid cells with non-significant Kendall τ ($P > 0.05$) were not included in the figures for visual purposes.

Changes in vegetation, such as greening or browning, can alter the dynamic equilibrium of the atmosphere-soil-vegetation interaction, leading to ecohydrological effects that impact ecosystem sustainability². While our study focused on the influence of climatic factors on resilience changes, further research is necessary to fully understand the underlying mechanisms driving the inconsistent changes observed in vegetation dynamics and resilience. Previous studies have highlighted the negative impacts of overplanting, the introduction of exotic plant species, and inadequate management practices on soil moisture in revegetated regions^{26,30,37,49}. Recently, an ecohydrological model demonstrated that the current vegetation cover in many parts of the Loess Plateau (average 0.48) has already exceeded the equilibrium vegetation cover determined by climate (average 0.43), particularly in the central and eastern areas²⁶. Interestingly, the regions exhibiting resilience loss in the second decade (Fig. 2f) aligned with the areas exceeding the climate-defined equilibrium vegetation cover²⁶. Moreover, we observed a shift from resilience gains to losses at a breakpoint coinciding with greening. This suggests the existence of a potential inflection point where greening no longer contributes to resilience gains. However, further investigation is needed to determine the specific levels of greening (density) and reasonable plant communities for optimal resilience.

Conclusions

Pervasive transitions in ecosystems have been observed and are expected to escalate in a changing world, highlighting the need to assess ecosystem resilience as a global priority^{9,12,14,35,50–52}. In this study, we evaluated vegetation dynamics and resilience in China's Loess Plateau from 2000 to 2020. Our findings reveal an overall greening trend in vegetated areas during this period, while resilience shifted from gains to losses in December 2010, marked by a breakpoint. This empirical evidence demonstrates that vegetation greening alone does not necessarily correspond to a consistent increase in resilience. Although further research is necessary to fully grasp the mechanisms driving resilience changes, our analysis suggests that warming and precipitation variability likely contribute to the resilience loss observed in the second decade.

Resilience indicators can offer valuable insights into vegetation states that might not be discernible through simple approaches like linear regression. Incorporating these indicators into ecological restoration assessments can guide the identification of priority regions with resilience loss, the determination of optimal vegetation density, and the selection of resilient species communities. To achieve more comprehensive ecosystem stewardship, we recommend integrating resilience indicators into assessments of ecological restoration effectiveness. This integration will provide a deeper understanding of ecosystem dynamics and enhance decision-making processes for ecological restoration practices.

Methods

Study area. The Loess Plateau is located in central China and is the largest and thickest loess deposit in the world, spanning ~640,000 km² (Supplementary Fig. 1). It is characterized by a temperate continental monsoon climate with an annual mean precipitation of 400 mm³⁷. The LP comprises arid, semi-arid, and semi-humid areas distributed from northwest to southeast, respectively, though the majority of the Loess Plateau is in a semi-arid zone³⁸. Due to cropland expansion, sparse vegetation, and the erosion susceptibility of loess, the Loess Plateau has historically faced severe soil erosion and land degradation^{38,53}. To restore the degraded landscape, the Chinese government implemented the Grain-to-Green Program in the Loess Plateau in

1999⁴⁰. Over more than two decades of ecological restoration efforts, significant greening has been reported in most areas of the Loess Plateau^{41–43}. However, despite these achievements in ecological restoration, there remain uncertainties regarding the vegetation ecosystems in the Loess Plateau, particularly in the face of rapid global environmental change³⁷. Specifically, there is limited knowledge about changes in vegetation resilience that occur alongside greening. Therefore, the objective of our study is to assess both vegetation dynamics and resilience from 2000 to 2020 and investigate whether resilience increases in conjunction with greening.

Data preparation. Monthly NDVI data with a resolution of 1 km from February 2000 to December 2020 were obtained from the Moderate Resolution Imaging Spectroradiometer sensor (MOD13A3 Version 6). This dataset was utilized to analyze both vegetation dynamics and resilience in the Loess Plateau due to its high spatial resolution and continuous measurements by a single sensor. Next, the collected NDVI data were processed to derive kNDVI using a simplified Eq. (1)⁴⁵. kNDVI is a newly proposed unified vegetation index that has demonstrated closer alignment with primary productivity, resistance to saturation, bias, and phenological cycles, as well as improved robustness to noise and instability across spatial and temporal scales compared to alternative products such as NDVI and near-infrared reflectance of vegetation^{5,45}. Therefore, we chose kNDVI as the preferred metric to evaluate the state of the vegetation ecosystem in this study.

$$kNDVI = \tanh(NDVI^2) \quad (1)$$

A key assumption of resilience indicators based on critical slowing down is that changes in the ecosystem should occur naturally rather than being forced by human land-use changes over time^{7,36}. To minimize the influence of anthropogenic land use on resilience signals, we excluded anthropogenic and non-vegetated landscapes (e.g., urban areas, cropland)^{7,36}. We focused on vegetated land, specifically grassland and forest, that remained unchanged from 2000 to 2020 based on a land cover dataset (Supplementary Fig. 1). The land cover data, obtained from Yang et al.⁵⁴, had a spatial resolution of 30 m, which we resampled to a 1 km resolution using the NEAREST method in ArcGIS desktop⁵⁵. China's national boundary was obtained from the standard map service of China's Ministry of Natural Resources (<http://bzdt.ch.mnr.gov.cn/>). The Loess Plateau boundary data was obtained from Loess Plateau SubCenter, National Science & Technology Infrastructure of China, National Earth System Science Data Sharing Infrastructure⁵⁶. The Yellow River shapefile data was acquired from Resource and Environment Science and Data Center⁵⁷.

To calculate the resilience metric AR(1), equidistant data is required¹⁹. Therefore, we examined the missing values in each kNDVI time series and found that locations with complete kNDVI time series accounted for 99.03% of the vegetated land (Supplementary Fig. 2). Interpolating missing values could introduce spurious changes in AR(1), as the interpolated values may resemble the existing values rather than representing any actual change in the underlying process or resilience^{7,19}. Given that locations with incomplete kNDVI time series constituted only a small fraction of the vegetated land (0.97%), we simply excluded these areas and instead focused solely on locations with complete kNDVI time series when calculating resilience metrics.

To investigate the influence of climate factors on vegetation resilience, we used monthly precipitation, temperature, and potential evapotranspiration data obtained from the National Earth System Science Data Center and the National Science & Technology Infrastructure of China⁵⁸. These data were available

at a spatial resolution of 1 km for the period 2000–2020. The aridity index was quantified as precipitation divided by potential evapotranspiration⁵⁹. Higher values indicate more humid conditions, while lower values indicate higher aridity⁵⁹. To assess the impact of the mean climate state on vegetation resilience, we calculated the mean values of precipitation, temperature, potential evapotranspiration, and aridity index within a sliding window, similar to the approach used for calculating AR(1). Likewise, we calculated the variability of precipitation and temperature within the same sliding window to investigate the impact of climate variability on vegetation resilience.

Vegetation dynamics and resilience. The rate of return to equilibrium, following a (small) perturbation, tends to slow down as systems approach critical transitions¹⁷. This phenomenon, known as “critical slowing down”, can be detected by examining changes in the correlation structure of a time series¹⁹. The simplest measure of slowing down is autocorrelation, specifically autocorrelation at-lag-1. An increase in autocorrelation at-lag-1 indicates that the system’s state has become increasingly similar between consecutive observations, reflecting a decline in recovery rates¹⁹. There are various methods to calculate autocorrelation at-lag-1^{17–19}. In this study, we employ a conditional least-squares method to fit a linear autoregressive model of order 1, denoted as AR(1), using the following Eq. (2)¹⁹:

$$Z_{t+1} = AR(1)Z_t + \varepsilon_t \quad (2)$$

Where Z_t is the subset of the ecological state series (i.e., kNDVI time series in this study). Z_{t+1} is the first-order lag time series. AR(1) is the autoregressive coefficient. ε_t is the residuals obtained by the ordinary least-squares method. The AR(1) provides a robust indicator for “critical slowing down” before bifurcation-induced transitions and has been widely used in vegetation resilience assessments^{6,7,10,11,36}.

Prior to estimating the resilience metrics, it is necessary to remove trends from the kNDVI time series^{11,19}. Trends indicate nonstationary conditions that can potentially impact the resilience metrics in unwanted ways¹⁹. We utilized the STL (Seasonal and Trend decomposition using Loess) decomposition technique, implemented through the `stl()` function in the ‘stats’ package (v4.2.1) in R⁶⁰. This decomposition method separates the kNDVI time series in each grid cell into an overall trend, a seasonal component, and a residual component¹¹. For our resilience estimation, we exclusively utilized the STL residual component, representing the de-seasoned and de-trended kNDVI time series^{11,36}. In the `stl()` function, we kept the `s.window` parameter as ‘periodic’ and varied the `t.window` (trend window) parameter to test the robustness of resilience estimates to the choice of trend window. Note that we compared analyses using both the `stl()` function and the `stlplus()` function and obtained the same results (Supplementary Fig. 3). To estimate the vegetation resilience indicator AR(1), we employed the `ar.ols()` function from the ‘stats’ package (v4.2.1) in R⁶⁰. The AR(1) coefficient was measured using a sliding window with a length equal to 60 months, thereby generating a time series of AR(1) coefficients for each location.

To assess the robustness of the resilience estimates, we adjusted our investigation in three ways to estimate how our results may have been influenced by our method of analysis. Firstly, we varied the size of the trend window (`t.window` parameter) in the `stl()` function, and the outcomes of alternative detrended time series can be found in Supplementary Fig. 4. Secondly, we explored the impact of varying the sliding window length during the calculation of AR(1) using the `ar.ols()` function, and the results for different sliding window lengths are depicted in

Supplementary Fig. 5. Lastly, we examined changes in variance over time as an additional indicator of critical slowing down to compare against AR(1)^{18,61}. The findings for the variance indicator are presented in Supplementary Figs. 6, 7. These results convincingly indicate that our resilience estimates remain robust across different detrending methods, sliding window lengths, and resilience indicators.

In this study, vegetation dynamics refer to the changes in the mean state of vegetation ecosystems. To facilitate a comparison between vegetation dynamics and resilience changes, we computed the mean kNDVI time series within the same sliding windows as the AR(1), ensuring temporal alignment. This sliding window approach generated a time series representing the mean values of kNDVI. In addition to calculating the resilience metric AR(1) and mean kNDVI values for the entire 2000–2020 period, we also performed similar calculations for two consecutive and independent decades: 2000–2010 (the first decade) and 2011–2020 (the second decade). This facilitated a comparative analysis. To assess regional changes, we calculated the mean AR(1) and kNDVI for all grid cells at each time point, transforming the data from a grid-scale to a regional-scale format (Fig. 1a). In addition, we calculated the 95% confidence intervals to measure uncertainty associated with the mean values.

Analyses. To assess the trends of AR(1), we employed Kendall’s τ , a rank correlation coefficient commonly utilized for estimating resilience tendencies in recent studies^{5,6,11}. The advantage of using Kendall’s τ is its ability to make resilience trends comparable across different regions⁶. We used the `cor.test()` function with the Kendall method from the R package ‘stats’ (v4.2.1) and set the confidence level at 0.95 to measure the tendency of AR(1)⁶⁰. A significant positive (negative) value of Kendall’s τ ($P < 0.05$) indicates an increasing (decreasing) tendency of AR(1), which corresponds to a loss (gain) of resilience and an increased (decreased) risk of critical transitions when exposed to disturbances. For comparison, we employed the same method to determine the tendency of the mean kNDVI time series. A significant positive (negative) value of Kendall’s τ ($P < 0.05$) indicates an increasing (decreasing) trend of mean kNDVI values, corresponding to a greening (browning) trend.

We utilized the ‘bfast’ function in R package ‘bfast’ (v1.6.1) to detect abrupt change points in the mean AR(1) time series at a regional scale⁶². Given that the mean AR(1) time series exhibited a U-shape pattern (Fig. 1a), we set the ‘breaks’ parameter to 1 to limit the maximum number of breaks to be calculated. To analyze changes in vegetation dynamics and resilience at the grid scale, we used histogram plots to examine the frequency distribution of Kendall τ values for the kNDVI and AR(1) time series. Specifically, we compared the data for two distinct decades, namely 2000–2010 and 2011–2020 (Fig. 1b, c). The spatial patterns and area proportions for the Kendall τ values of the kNDVI and AR(1) time series were depicted in Fig. 2. To examine the relationships between vegetation greening/browning and resilience, we first created a cumulative density distribution plot between AR(1) Kendall τ and kNDVI Kendall τ (Fig. 1d–f). In addition, we analyzed the temporal correlations between AR(1) series and kNDVI series at each grid cell using the ‘cor.test()’ function with the Pearson method⁶⁰ (Fig. 3).

To analyze changes in vegetation resilience with respect to climatic factors, we initially calculated the annual mean values of precipitation, temperature, potential evapotranspiration, and aridity index from 2000 to 2020. These climate variables were divided into 50 gradients. Next, we determined the median value of the AR(1) Kendall τ within each climate gradient (Fig. 4). To investigate the impact of climate factors on vegetation resilience,

we used multiple linear regression models to quantify the direction and intensity of the influence of each climate variable on the AR(1)¹⁴. A separate multiple linear regression model was constructed for each grid location, with the AR(1) time series as the dependent variable and 6 explanatory variables including mean precipitation, mean temperature, precipitation variability, temperature variability, mean potential evapotranspiration, and mean aridity index. The `scale()` function in R package base (v4.2.1) was applied to scale the variables to a mean of 0 and reduce unit variance to improve model convergence⁶⁰. In addition, we utilized the `'calc.relimp()'` function from the R package `'relaimpo'` (v2.2.6) to determine the relative importance of factors in the regression models⁶³. Finally, we extracted regression coefficients, *P* values, and relative importance for each environmental factor. Vegetation grids with non-significant regression coefficients were excluded from subsequent analysis (Fig. 5). The spatial patterns of regression coefficients and relative importance for each climatic variable are shown in Supplementary Figs. 8, 9. All analyses mentioned above were conducted in R environment (version 4.2.2)⁶⁰.

Data availability

Monthly NDVI data with a resolution of 1 km from February 2000 to December 2020 were acquired from MODIS (MOD13A3 Version 6, <https://lpdaac.usgs.gov/products/mod13a3v006/>). Land use/cover data with a 30 m resolution in 2000 and 2020 was obtained from Zenodo (<https://zenodo.org/record/5210928>). Monthly precipitation, temperature, and potential evapotranspiration with a resolution of 1 km from January 2000 to December 2020 were acquired from National Earth System Science Data Center, National Science & Technology Infrastructure of China: precipitation (<http://www.geodata.cn/data/datadetails.html?dataguid=192891852410344&docId=1069>), temperature (<http://www.geodata.cn/data/datadetails.html?dataguid=164304785536614&docId=1737>), potential evapotranspiration (<http://loess.geodata.cn/data/datadetails.html?dataguid=34595274939620&docId=69>). China's national boundary (GS(2020)4619) was obtained from the standard map service of China's Ministry of Natural Resources (<http://bzdt.ch.mnr.gov.cn/>). The Loess Plateau boundary data was obtained from Loess Plateau SubCenter, National Science & Technology Infrastructure of China, National Earth System Science Data Sharing Infrastructure (<http://loess.geodata.cn/datapplication/OrderStepList.html?dataguid=23394955913595>). The Yellow River shapefile data was obtained from Resource and Environment Science and Data Center (<https://www.resdc.cn/DOI/DOLaspx?DOIID=44>).

Code availability

Code for analysis and drawing main figures can be found at https://github.com/geowaa/Vegetation_Greening_Resilience.

Received: 14 March 2023; Accepted: 13 September 2023;

Published online: 22 September 2023

References

- Li, W. et al. Widespread increasing vegetation sensitivity to soil moisture. *Nat. Commun.* **13**, 1–9 (2022).
- Piao, S. et al. Characteristics, drivers and feedbacks of global greening. *Nat. Rev. Earth Environ.* **1**, 14–27 (2020).
- Strand, J. et al. Spatially explicit valuation of the Brazilian Amazon Forest's Ecosystem Services. *Nat. Sustain.* **1**, 657–664 (2018).
- Chen, C. et al. China and India lead in greening of the world through land-use management. *Nat. Sustain.* **2**, 122–129 (2019).
- Forzieri, G., Dakos, V., McDowell, N. G., Ramdane, A. & Cescatti, A. Emerging signals of declining forest resilience under climate change. *Nature* **608**, 534–539 (2022).
- Feng, Y. et al. Reduced resilience of terrestrial ecosystems locally is not reflected on a global scale. *Commun. Earth Environ.* **2**, 88 (2021).
- Smith, T., Traxl, D. & Boers, N. Empirical evidence for recent global shifts in vegetation resilience. *Nat. Clim. Chang.* **12**, 477–484 (2022).
- Hu, Y. et al. Changes and influencing factors of ecosystem resilience in China. *Environ. Res. Lett.* **18**, 094012 (2023).
- Hirota, M., Holmgren, M., Van Nes, E. H. & Scheffer, M. Global resilience of tropical forest and savanna to critical transitions. *Science (80-)* **334**, 232–235 (2011).
- Verbesselt, J. et al. Remotely sensed resilience of tropical forests. *Nat. Clim. Chang.* **6**, 1028–1031 (2016).
- Boulton, C. A., Lenton, T. M. & Boers, N. Pronounced loss of Amazon rainforest resilience since the early 2000s. *Nat. Clim. Chang.* **12**, 271–278 (2022).
- McDowell, N. G. et al. Pervasive shifts in forest dynamics in a changing world. *Science (80-)* **368**, eaaz9463 (2020).
- Khoury, S. & Coomes, D. A. Resilience of Spanish forests to recent droughts and climate change. *Glob. Chang. Biol.* **26**, 7079–7098 (2020).
- Berdugo, M., Gaitan, J. J., Delgado-Baquerizo, M., Crowther, T. W. & Dakos, V. Prevalence and drivers of abrupt vegetation shifts in global drylands. *Proc. Natl. Acad. Sci. USA.* **119**, 1–10 (2022).
- Fernández-Martínez, M. et al. Diagnosing destabilization risk in global land carbon sinks. *Nature* **615**, 848–853 (2023).
- Dakos, V., Carpenter, S. R., van Nes, E. H. & Scheffer, M. Resilience indicators: Prospects and limitations for early warnings of regime shifts. *Philos. Trans. R. Soc. B Biol. Sci.* **370**, 1–10 (2015).
- Scheffer, M. et al. Early-warning signals for critical transitions. *Nature* **461**, 53–59 (2009).
- Scheffer, M., Carpenter, S. R., Dakos, V. & Van Nes, E. H. Generic Indicators of Ecological Resilience: Inferring the Chance of a Critical Transition. *Annu. Rev. Ecol. Evol. Syst.* **46**, 145–167 (2015).
- Dakos, V. et al. Methods for detecting early warnings of critical transitions in time series illustrated using simulated ecological data. *PLoS ONE* **7**, e41010 (2012).
- Arani, B. M. S., Carpenter, S. R., Lahti, L., Van Nes, E. H. & Scheffer, M. Exit time as a measure of ecological resilience. *Science (80-)* **372**, eaay4895 (2021).
- Ratajczak, Z. et al. Reintroducing bison results in long-running and resilient increases in grassland diversity. *Proc. Natl. Acad. Sci. USA.* **119**, 1–7 (2022).
- Braun, D. M., Washburn, J. D. & Wood, J. D. Enhancing the resilience of plant systems to climate change. *J. Exp. Bot.* **74**, 2787–2789 (2023).
- Freund, S. M. et al. Plant functional groups and species contribute to ecological resilience a decade after woodland expansion treatments. *Ecosphere* **12**, e03325 (2021).
- Lortie, C. J., Filazzola, A., Westphal, M. & Butterfield, H. S. Foundation plant species provide resilience and microclimatic heterogeneity in drylands. *Sci. Rep.* **12**, 1–8 (2022).
- Gazol, A. et al. Forest resilience to drought varies across biomes. *Glob. Chang. Biol.* **24**, 2143–2158 (2018).
- Zhang, S. et al. Excessive Afforestation and Soil Drying on China's Loess Plateau. *J. Geophys. Res. Biogeosci.* **123**, 923–935 (2018).
- Feng, X. et al. Revegetation in China's Loess Plateau is approaching sustainable water resource limits. *Nat. Clim. Chang.* **6**, 1019–1022 (2016).
- Liang, W. et al. Quantification of the ecosystem carrying capacity on China's Loess Plateau. *Ecol. Indic.* **101**, 192–202 (2019).
- Cui, J. et al. Global water availability boosted by vegetation-driven changes in atmospheric moisture transport. *Nat. Geosci.* <https://doi.org/10.1038/s41561-022-01061-7> (2022).
- Liang, H. et al. Soil moisture decline following the plantation of Robinia pseudoacacia forests: Evidence from the Loess Plateau. *For. Ecol. Manage.* **412**, 62–69 (2018).
- Cao, S. et al. Excessive reliance on afforestation in China's arid and semi-arid regions: Lessons in ecological restoration. *Earth-Sci. Rev.* **104**, 240–245 (2011).
- Zemp, D. C. et al. Self-amplified Amazon forest loss due to vegetation-atmosphere feedbacks. *Nat. Commun.* **8**, 14681 (2017).
- Fischer, J., Riechers, M., Loos, J., Martín-Lopez, B. & Temperton, V. M. Making the UN Decade on Ecosystem Restoration a Social-Ecological Endeavour. *Trends Ecol. Evol.* **36**, 20–28 (2021).
- Tedesco, A. M. et al. Beyond ecology: ecosystem restoration as a process for social-ecological transformation. *Trends Ecol. Evol.* **38**, 643–653 (2023).
- Brando, P. M. et al. Abrupt increases in Amazonian tree mortality due to drought-fire interactions. *Proc. Natl. Acad. Sci. USA.* **111**, 6347–6352 (2014).
- Smith, T. & Boers, N. Global vegetation resilience linked to water availability and variability. *Nat. Commun.* **14**, 1–11 (2023).
- Fu, B., Wu, X., Wang, Z., Wu, X. & Wang, S. Coupling human and natural systems for sustainability: experience from China's Loess Plateau. *Earth Syst. Dyn.* **13**, 795–808 (2022).
- Fu, B. et al. Hydrogeomorphic Ecosystem Responses to Natural and Anthropogenic Changes in the Loess Plateau of China. *Annu. Rev. Earth Planet. Sci. is online earth.annualreviews.org* **45**, 223–266 (2017).
- Chen, Y. et al. Balancing green and grain trade. *Nat. Geosci.* **8**, 739–741 (2015).
- Bryan, B. A. et al. China's response to a national land-system sustainability emergency. *Nature* **559**, 193–204 (2018).
- Yu, Y., Zhao, W., Martínez-Murillo, J. F. & Pereira, P. Loess Plateau: from degradation to restoration. *Sci. Total Environ.* **738**, 140206 (2020).
- Naeem, S. et al. Both climate and socioeconomic drivers contribute to vegetation greening of the Loess Plateau. *Sci. Bull.* **66**, 1160–1163 (2021).

43. Wu, X., Wang, S., Fu, B., Feng, X. & Chen, Y. Socio-ecological changes on the Loess Plateau of China after Grain to Green Program. *Sci. Total Environ.* **678**, 565–573 (2019).
44. Deng, L. & Shangquan, Z. High quality developmental approach for soil and water conservation and ecological protection on the loess plateau. *Front. Agric. Sci. Eng.* **8**, 501–511 (2021).
45. Camps-Valls, G. et al. A unified vegetation index for quantifying the terrestrial biosphere. *Sci. Adv.* **7**, 1–11 (2021).
46. Liu, Y., Kumar, M., Katul, G. G. & Porporato, A. Reduced resilience as an early warning signal of forest mortality. *Nat. Clim. Chang.* **9**, 880–885 (2019).
47. Kéfi, S., Dakos, V., Scheffer, M., Van Nes, E. H. & Rietkerk, M. Early warning signals also precede non-catastrophic transitions. *Oikos* **122**, 641–648 (2013).
48. Zeng, Y. et al. Optical vegetation indices for monitoring terrestrial ecosystems globally. *Nat. Rev. Earth Environ.* **3**, 477–493 (2022).
49. Chen, L., Wang, J., Wei, W., Fu, B. & Wu, D. Effects of landscape restoration on soil water storage and water use in the Loess Plateau Region, China. *For. Ecol. Manage.* **259**, 1291–1298 (2010).
50. Van Der Bolt, B., Van Nes, E. H., Bathiany, S., Vollebregt, M. E. & Scheffer, M. Climate reddening increases the chance of critical transitions. *Nat. Clim. Chang.* **8**, 478–484 (2018).
51. Ratajczak, Z. et al. Abrupt Change in Ecological Systems: Inference and Diagnosis. *Trends Ecol. Evol.* **33**, 513–526 (2018).
52. Beaugrand, G., Edwards, M., Brander, K., Luczak, C. & Ibanez, F. Causes and projections of abrupt climate-driven ecosystem shifts in the North Atlantic. *Ecol. Lett.* **11**, 1157–1168 (2008).
53. Wu, X. et al. Evolution and effects of the social-ecological system over a millennium in China's loess plateau. *Sci. Adv.* **6**, eabc0276 (2020).
54. Yang, J. & Huang, X. The 30m annual land cover dataset and its dynamics in China from 1990 to 2019. *Earth Syst. Sci. Data* **13**, 3907–3925 (2021).
55. ESRI. ArcGIS Desktop: release 10.4.1 (Environmental Systems Research Institute, 2016).
56. Loess Plateau SubCenter, National Science & Technology Infrastructure of China, National Earth System Science Data Sharing Infrastructure (<http://www.geodata.cn>).
57. Xu X. & Zhuang D. Automated extraction of drainages in China based on DEM in GIS environment. in *IGARSS 2003. 2003 IEEE International Geoscience and Remote Sensing Symposium. Proceedings (IEEE Cat. No.03CH37477)* 5 3344–3346 (IEEE, 2004).
58. No Title. *National Earth System Science Data Center, National Science & Technology Infrastructure of China* (<http://www.geodata.cn>).
59. Zomer, R. J., Xu, J. & Trabucco, A. Version 3 of the Global Aridity Index and Potential Evapotranspiration Database. *Sci. Data* **9**, 1–15 (2022).
60. R Core Team. R: A language and environment for statistical computing. *R Foundation for Statistical Computing* <http://www.R-project.org> (2019).
61. Carpenter, S. R. & Brock, W. A. Rising variance: A leading indicator of ecological transition. *Ecol. Lett.* **9**, 311–318 (2006).
62. Verbesselt, J., Hyndman, R., Newnham, G. & Culvenor, D. Detecting trend and seasonal changes in satellite image time series. *Remote Sens. Environ.* **114**, 106–115 (2010).
63. Grömping, U. Relative importance for linear regression in R: The package relaimpo. *J. Stat. Softw.* **17**, 1–27 (2006).

Acknowledgements

This study was supported by the National Natural Science Foundation of China (41930649).

Author contributions

B.F. and Z.W. conceived and designed the study. Z.W. produced and analyzed the results and led the writing of the paper. B.F., X.W., Y.L., Y.F., S.W., F.W., and L.Z. commented and edited the paper. All authors contributed to interpreting the results and improving the paper.

Competing interests

The authors declare no competing interests.

Additional information

Supplementary information The online version contains supplementary material available at <https://doi.org/10.1038/s43247-023-01000-3>.

Correspondence and requests for materials should be addressed to Bojie Fu.

Peer review information *Communications Earth & Environment* thanks the anonymous reviewers for their contribution to the peer review of this work. Primary Handling Editors: Heike Langenberg, Alienor Lavergne. A peer review file is available.

Reprints and permission information is available at <http://www.nature.com/reprints>

Publisher's note Springer Nature remains neutral with regard to jurisdictional claims in published maps and institutional affiliations.



Open Access This article is licensed under a Creative Commons Attribution 4.0 International License, which permits use, sharing, adaptation, distribution and reproduction in any medium or format, as long as you give appropriate credit to the original author(s) and the source, provide a link to the Creative Commons licence, and indicate if changes were made. The images or other third party material in this article are included in the article's Creative Commons licence, unless indicated otherwise in a credit line to the material. If material is not included in the article's Creative Commons licence and your intended use is not permitted by statutory regulation or exceeds the permitted use, you will need to obtain permission directly from the copyright holder. To view a copy of this licence, visit <http://creativecommons.org/licenses/by/4.0/>.

© The Author(s) 2023